journal of the mechanical behavior of biomedical materials 133 (2022) 105324

Contents lists available at ScienceDirect

Journal of the Mechanical Behavior of Biomedical Materials

journal homepage: www.elsevier.com/locate/jmbbm

Diatomaceous earth as a drug-loaded carrier in a glass-ionomer cement

Magdalena Łępicka [a,*], Magdalena Rodziewicz [a], Michał Kawalec [a], Klaudia Nowicka [a], Yurii Tsybrii [b], Krzysztof Jan Kurzydłowski [a]

[a] Institute of Mechanical Engineering, Faculty of Mechanical Engineering, Bialystok University of Technology, Wiejska 45C St., 15-352, Bialystok, Poland
[b] Institute of Mechanics and Machine Design, Faculty of Mechanical Engineering and Ship Technology, Gdansk University of Technology, G. Narutowicza 11/12 St., 80-233, Gdansk, Poland

ARTICLE INFO

Keywords:
Glass-ionomer cement
Diatomaceous earth
Drug-loaded agent
Natural material
Drug delivery

ABSTRACT

The effect of a natural filler (diatomaceous earth [DE], a promising drug-delivery agent) and its content was investigated on the performance of a model glass-ionomer cement (GIC). Three sample series, differing in DE content (0, 2.5 and 5 wt%), were prepared using a commercial GIC as a matrix (3M Ketac Molar Easymix). The resultant surface microhardness and roughness, wear performance, and compressive strength of the samples were measured after the samples had been stored in deionized water at 37°C for a fixed time. Moreover, the film thickness was tested for the freshly mixed samples. The numerical data was subjected to statistical analysis, in order to test the null hypotheses of the equality of the measured properties between the reference and the DE-modified samples. According to the results, diatomaceous earth particles are uniformly distributed in the GIC matrix, and the cavities of frustules tend to be filled with the GIC. This translates into the observed performance of the DE-loaded GIC. Compared with the reference material (0 wt% DE), the surface microhardness (2.5 wt% DE, $p = 0.014$; 5 wt% DE, $p = 0.005$) and roughness (e.g. Ra; 2.5 wt% DE, $p = 0.003$; 5 wt% DE, $p < 0.001$) are increased. No effect on the wear performance ($p = 0.530$ and 0.256, respectively) or compressive strength ($p = 0.514$) was noticed in the case of DE partially substituting the glass phase. Based on the study results, it is evidenced that diatom frustules are a suitable filler for application in conventional glass-ionomer cements as the glass-substituting drug-loaded carrier. Notably, however, the surface finish method of the DE-filled materials needs development.

1. Introduction

The first dental filling of modern dentistry was any metal sufficiently soft to mold into the cavity, for instance, silver or tin. This evolved to dental amalgams comprising metals including silver, tin, copper, and mercury. Silicate dental cements were created for dental filling and the bonding of other dental restorations in the mid-1920s (Lohbauer, 2009). Apparently, amalgam is still a frequently used filling material in several low-income countries as a consequence of its cost-effectiveness (Worthington et al., 2021). However, concerns regarding mercury release in the human body, its allergic and toxic potential upon release, and finally the spread and disposal of mercury and its compounds in the environment, have contributed to the decrease of use of the amalgam in dentistry. Notably, decommissioning of amalgam fillings is enforced also by the Minamata Convention on Mercury, established by The United Nations Environment Programme. This treaty intends to protect human health and the environment from emissions and releases of mercury and mercury compounds caused by humans, also in dentistry (Kielbassa et al., 2016, 2017), and proposes nine measures to phase down the use of dental amalgam (Fisher et al., 2018). In fact, there are effective mercury-free alternatives at present, which have the extra aesthetic advantage of being the same color as the tooth, e.g. composite resins. Therefore, the proportion of amalgam fillings is decreasing. Comparing composite resins with GICs, it should be noticed that although composites help with the esthetics problem, giving teeth a natural, smooth, unblemished look, they suffer from several drawbacks. The challenges are polymerization shrinkage, postoperative sensitivity, and the demand for perfection and technical proficiency of clinicians. In fact, a significant development was made over the last decades to improve the adhesion of these composite resins, which is one key factor in restorative dentistry (Sofan et al., 2017). However, GICs still remain clinically attractive dental materials, having the extra benefits of strong adhesion

* Corresponding author.
E-mail address: m.lepicka@pb.edu.pl (M. Łępicka).

https://doi.org/10.1016/j.jmbbm.2022.105324
Received 14 April 2022; Received in revised form 9 June 2022; Accepted 13 June 2022
Available online 15 June 2022

to the moist tooth surface, as well as anticariogenic properties, attributed to the release of fluoride (Lohbauer, 2009). Nevertheless, the application of GICs in mechanically loaded situations is questioned as a consequence of their low fracture strength, toughness and wear resistance (Lohbauer, 2009). However, in some cases they have shown a clinical performance significantly higher than composite resins, e.g. in regard to retention in restorations of non-carious cervical lesions (Lohbauer, 2009) or in restorations placed in primary teeth using the ART approach (Ersin et al., 2006).

Glass-ionomer cements have a range of compositions, but the major constituents are alumina, silica, and calcium. A source of fluoride, such as fluorite, is also usually incorporated to offer protection against tooth decay. More minerals can also be added into the GIC to boost demineralization and prevent acidification. Moreover, the glass ionomer may be incorporated with resin for extra strength as well as to reduce the sensitivity to the presence of moisture on placement (Gao et al., 2000). GICs signify a very flexible dental restoration solution, as the physical properties of GIC can be altered to match a particular dental application by modifying the ratios of the constituent chemicals (Lohbauer, 2009). Recently, bioactive glass has been used for making GIC (Matsuya et al., 1999). Resin-modified GIC comprising bioactive glass was demonstrated to result in a thick uniform layer of mineralization on the restoration–dentin interface (Prabhakar et al., 2010), enhance the mechanical properties of a filling (Khvostenko et al., 2013), and reduce the incidence of secondary tooth decay at the restoration margins (Khvostenko et al., 2016).

Another trend observed in today's conservative dentistry is the development of bio-inspired dental filling (Khvostenko et al., 2016) or at least the use of natural compounds for the development of dental fillings (Lavigueur and Zhu, 2012). Of note also are drug-delivery systems being developed for dental applications. In fact, using antibiotics or other bioactive agents combined with drug carrier systems is a promising approach in the treatment and control of dental diseases (Ahmad et al., 2008; Liang et al., 2020; Ficai et al., 2017; Makvandi et al., 2021). Drug delivery systems seem to be especially desirable where there is limited access to dental care, which is still the case in less developed countries.

Apparently, diatomaceous biosilica and, more commonly, diatomaceous earth (DE) seem to be very promising GIC additives. Diatomaceous earth is a naturally occurring resource consisting of fossilized remains of diatoms, while diatomaceous biosilica is extracted from diatom biomasses (microalgaes). Chemically, their main ingredient is an inorganic polymer–amorphous silica (SiO_2) which correlates with the GIC composition. Both species are three-dimensional porous structures with a very large surface area and a typical size of frustules (particles) ranging from 10 μm to 200 μm. Most importantly, amorphous silica is not toxic and it is even advised to consume diatomaceous earth as it is considered to have a beneficial health effect. Another very promising feature is that the biosilica frustules can act as a biocarrier for drug-delivery applications (Delasoie and Zobi, 2019; Aw et al., 2012, 2013).

Nevertheless, theoretical expectations need experimental verification. Herein, the aim of the study was to experimentally verify the effect of incorporating diatomaceous earth particles on the performance of a conventional glass-ionomer cement. A set of null hypotheses on the lack of influence of the addition of diatomaceous earth on the crucial performance properties, which are: surface microhardness ($H_{0\text{-}1}$), compressive strength ($H_{0\text{-}2}$), film thickness ($H_{0\text{-}3}$), surface roughness ($H_{0\text{-}4}$), and tribological performance ($H_{0\text{-}5}$), were tested. These hypotheses were tested against the alternative hypotheses of a difference ($H_{A\text{-}1}$ to $H_{A\text{-}5}$) in comparison with a commercial GIC.

2. Materials and methods

2.1. Materials

Commercial 3M ESPE Ketac Molar Easymix (3M, St. Paul, USA) was used as the glass-ionomer cement (GIC). The chemical composition of this product is given in the Supplementary materials (Table S1). Diatomaceous earth Perma-Guard (CAS 61790-53-2, Fossil Shell Flour, Perma-Guard; Bountiful, USA), containing >99.9% of amorphous uncalcined silica, was used after drying under vacuum for 24 h at 80 °C.

2.2. Sample preparation

Reference samples were prepared following the procedure given by the manufacturer. Briefly, a fixed quantity of both glass-ionomer phases – glass powder and liquid, was hand-mixed at room temperature until full agglutination, and loaded into a mold. The time from contact of the two phases to loading of the mold did not exceed 180 s. After filling the molds, the samples were transferred to a laboratory cabinet and stored at 37 °C and a relative humidity of 90%. The glass powder to liquid weight ratio was fixed at 3.1:1.

Two series of the glass-ionomer cement filled with diatomaceous earth (GIC/DE) were prepared similarly to the reference material. However, part (2.5 or 5 wt%) of the powder ingredient was substituted with the respective amount of the DE and mixed with the remaining glass to a uniform mixture. Next, the liquid ingredient was added and mixed in thoroughly. Molds were filled with the prepared materials within 180 s counting from the liquid addition. Again, after filling, the molds were transferred to a laboratory cabinet, in which a temperature of 37 °C and relative humidity of 90% was maintained. As a result, three sample series were obtained containing: (1) 0 wt% of DE (reference), (2) 2.5 wt% of DE and (3) 5 wt% of DE.

The samples were prepared in the shape of disks with diameter 15 mm × height 2 mm (for microhardness, surface roughness, tribological performance tests), and diameter 4 mm × height 6 mm (for the compressive strength test). All three series of samples were stored at 36 °C in a laboratory incubator at a relative humidity > 95% after preparation. Laboratory tests were carried out at least 24 h after setting of the cement, except for the layer thickness measurements, for which the samples were mixed immediately before testing.

2.3. Methods

2.3.1. Microscopic observations

The microscopic observations were done with the use of a scanning electron microscope (Scios 2 DualBeam SEM-FIB, Thermo Fisher Scientific; Waltham, USA). During the studies, the backscatter electron (T1) in-lens detector was used. The observations were done for all three sample series (0, 2.5 and 5 wt% DE, respectively). The morphology of the diatomaceous earth particles, the cross-sections of the glass-ionomer samples, as well as the morphology of the wear tracks obtained in tribological studies were included in the study.

2.3.2. Microhardness

A Vickers microhardness tester (MicVision VH-1, Sinowon; Dong Guan, China) was used for microhardness tests. The load was set at 200 gf (1.96 N). The measurements were taken for all the sample series at fixed time intervals: 24 h (1 day) and 7 days after specimen preparation. Between the measurements, the samples were stored at 37 °C in a laboratory incubator, in deionized water. For each sample type, n = 10 measurements were taken.

2.3.3. Compressive strength test

The compressive strength tests were carried out in accordance with ISO 9917–1 using a universal testing system (Bionix Table Top System, MTS Systems; Eden Prairie, USA). The sample was placed in such a way that its longitudinal axis coincided with the load axis. The crosshead speed was set to 0.005 mm/s. Based on the obtained data, the maximum compressive stress of the samples was calculated, using the formula:

$$\sigma_{max} = \frac{N_{max}}{A}$$

where:

σ_{max} – maximum compressive stress [MPa],
N_{max} – maximum compressive load [N],
A – area of the initial cross-section of a sample [mm^2].

For each sample type, 5 measurements were taken. According to ISO 9917–1, in at least 4 out of 5 of the tested samples the compressive strength of a glass-ionomer restorative material should be greater than or equal to 100 MPa.

2.3.4. Layer thickness

The requirements for measuring the layer thickness of glass-ionomers are given in ISO 9917–1. The aim of this test is to assess the applicability of the developed materials for fixing permanent dental restorations. According to the ISO 9917-1 standard, the layer thickness tests are carried out on a freshly mixed GIC, for dental materials that can be used, among others, for fixing crowns or bridges. The aim is to check that the resultant thickness of the cement is not too high, so that it will not influence the resultant height of a restoration.

The layer thickness measurements are performed on round or square glass samples, with a thickness greater than or equal to 5 mm, which results in a contact area of 200 ± 25 mm^2. The tests are carried out on testing machines capable of applying a compressive force of 150 N, with a tolerance of ±2 N. This force is used to mimic the forces which are applied during crown fitting. Before starting the tests, the thickness of the glasses used should be measured using a micrometer with a measuring tolerance of at least 2 μm.

The layer thickness was tested using the universal testing machine (MTS Insight, MTS Systems; Eden Prairie, USA) according to ISO 9917–1. Glass slides were ultrasonically cleaned with acetone and deionized water before the measurements. Then, the glass samples were dried at 120 °C and combined into pairs. The thickness of the two adjacent slides (in pairs) was measured with a micrometer. Fresh, cuboid samples (15 × 15 × 5 mm^3, length × width × thickness, respectively) were prepared for the tests by weighing the appropriate amount of glass powder, a liquid based on polyacids and DE filler (if used), followed by vigorous mixing on a paper blotter with a steel spatula. Next, a measured amount of the freshly mixed material was placed on a glass slide and gently pressed against it with a second piece of glass. Then, the sample was placed in the holder of the testing machine on a rubber, acting like a spring, ensuring a constant force acting on the material. The compressive force of 150 N was applied. Each time, in accordance with the normative requirements, the load was kept constant for 10 min. Then, the thickness of the sample (glass slide/cement/glass slide) was measured again. The thickness of the compressed layer of the glass-ionomer material was calculated using the following formula:

$$d_0 = d_2 - d_1$$

where:

d_0 – thickness of the glass-ionomer cement [mm],
d_1 – thickness of pair of glass slides before the test [mm],
d_2 – thickness of pair of glass slides, with the glass-ionomer material between them, after applying a load of 150 N for 10 min [mm].

For each sample type, n = 5 measurements were taken.

2.3.5. Surface roughness

The effect of introducing DE on the resultant surface roughness of the tested compositions was determined using a contact profilometer (Hommel Tester T1000, Hommel-Etamic; Jena, Germany). Measurements were carried out in accordance with the requirements of ISO 4288. The following values were determined: Ra (arithmetic mean roughness), Rz (greatest height of the roughness profile) and Rt (total profile height). For each series of samples, n = 5 measurements were taken.

2.3.6. Tribological performance

The friction tests were carried out on a biotribometer (UMT, Bruker; Billerica, USA). The test sample, placed in the holder, was reciprocating, while the ball – the counter sample – remained immobile (Fig. S1, Supplementary materials). The normal load was set to 5 N, the operating frequency of the friction pair was 1 Hz, and the length of the friction track was 500 μm. The test lasted 2 h, or 7200 s. The counter-sample, a corundum ball (Ø6 mm, Al_2O_3), was replaced with a new one before each subsequent test. This activity was performed in order to maintain the same frictional conditions for each sample. The tribological pair was lubricated with a commercial artificial mucin-rich saliva, Kserostemin (Aflofarm; Pabianice, Poland). For each sample series, n = 5 replications were done. During the frictional tests, the friction force vs. time signals were acquired with a frequency of 10 Hz. For all samples, the mean friction force was calculated.

Next, the frictional tracks were identified using a laser confocal microscope (CLSM, LEXT4000, Olympus; Tokyo, Japan) on the samples subjected to the frictional test. The volume of the removed material was measured. Moreover, the wear tracks that resulted from the frictional tests were subjected to additional microscopic observations with the use of a SEM-FIB system.

2.3.7. Statistical analysis

The data were statistically analyzed with Statistica 13.3.0 for Windows 10 (Statistica 13.3.0, Tibco Software; Palo Alto, USA). The normal distribution assumption was checked for all variables using the Shapiro–Wilk test. As the assumption was satisfied, the equality of variances was checked with Levene's test. After that, the data were subjected to individual analyses. If 3 or more groups were compared, a one-way ANOVA ($p \leq 0.05$), followed by Tukey's HSD post-hoc test ($p < 0.05$) for individual comparisons, was used. In other cases, t-tests were done ($p < 0.05$). However, for Ra and Rz roughness, as well as the volumetric wear measurements, in Levene's test, it was revealed that the variances were not uniform. Therefore, the roughness and volumetric wear data were analyzed with the use of the Welch F-test ($p \leq 0.05$), followed by the NIR post-hoc test ($p < 0.05$), for individual comparisons.

3. Results

3.1. Microscopic observations of diatomaceous earth and the as-received glass-ionomer samples

The Perma-Guard diatomaceous earth consists of fossil frustules of various sizes and shapes (Fig. 1a). In the raw material, intact frustules, along with agglomerates and broken diatom shells, are present (Fig. 1a). The length of a frustule does not exceed 40 μm, while its diameter is less than 20 μm (Fig. 1a and b). In Perma-Guard diatomite, the most abundant diatom frustule genus is *Aulacoseira* (Fig. 1b). These frustules are cylindrical, and form long straight chains (Kiss et al., 2012) of valves connected via linking spines (Fig. 1b). In the valves, a highly hierarchical structure of a shell is seen, where rows of small pores (areolae) are present.

The diatomaceous earth particles (Fig. 1a) were mixed with the selected glass-ionomer material. Compared with the control group (Fig. S2, Supplementary materials), in which a typical microstructure of a glass-ionomer cement was seen, after filling the GIC with DE, fossil frustules of different sizes and shapes were present (Fig. 1c). The fossil shells were homogeneously mixed within the glass-ionomer cement (Fig. 1c). The hydrogel matrix of the cement tended to fill the cavities of the frustules (Fig. 1d).

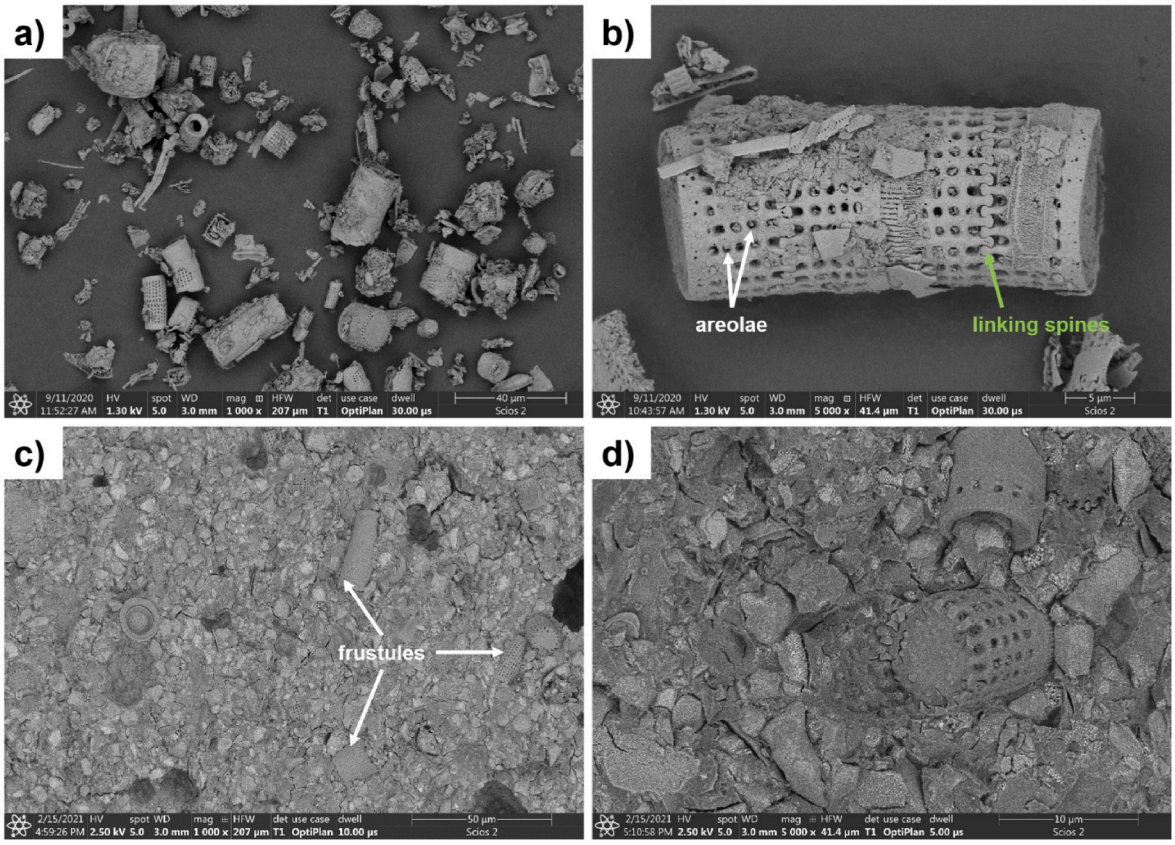

Fig. 1. SEM images of: (a–b) Perma-Guard diatomaceous earth; (a) the particles of the as-received diatomite; (b) mantle view of a single *Aulacoseira* frustule; (c–d) cross-section of the 5 wt% DE-filled GIC sample: frustules are seen along with glass particles and hydrogel matrix.

3.2. Microhardness

Microhardness tests were carried out on samples kept in a laboratory incubator for a fixed time – 1 or 7 days. The data obtained during the surface microhardness tests is presented in Table S2 (Supplementary materials). It can be noticed that, on day 1, a statistically significant difference in surface hardness was observed between the control and the DE-modified samples (Fig. 2). However, this effect was not as strong after 7 days of conditioning (Fig. 2). After 7 days of aging, compared with the control, only for samples modified with 5 wt% DE was a difference in surface microhardness seen. Nevertheless, when the results obtained at days 1 and 7 were compared, an increase in hardness was seen in each tested sample series (paired *t*-test, $p < 0.05$).

3.3. Compressive strength test

The compressive strength tests were conducted on samples kept, prior to the test, in a humid laboratory incubator at the temperature of 37 °C, according to the ISO 9917-1 standard requirements. The stiffness of the tested samples was similar considering the respective groups (see Fig. 3a, the displacement vs. compressive strength plots obtained for both groups: the control and the 5 wt% DE). This was evidenced by the similar angle of inclination of the curves, revealing the stress dependence on the displacement of the testing machine grips. Moreover, on the basis of the presented data, it was noticed that all the tested samples met the requirements set out in ISO 9917–1, relating to the minimum compressive strength of glass ionomers. All the tested samples achieved a compressive strength much higher than that specified in the standard, amounting to 100 MPa (Table S3, Supplementary materials). However, no statistically significant difference in compressive strength was observed between the reference and the DE-modified group (Fig. 3b).

3.4. Film thickness

In film thickness measurements, the tested material is mixed immediately before testing. Then, a drop of it is placed between two glass slides, compressed, and the resultant thickness of the GIC layer is measured with a micrometer. The findings from these tests are included in Table S4 (Supplementary materials). According to the obtained data (Fig. S3, Supplementary materials), the addition of DE in the tested GIC resulted in an increase in film thickness, measured according to ISO 9917–1. A statistical difference between the control and the DE-modified samples was seen only in the group where 5 wt% of DE was used (Fig. S3). However, it needs to be stressed that while the film thickness increased with the amount of DE used, even the control group did not meet the ISO 9917–1 requirements. Therefore, it can be stated that the proposed material will not find application as a luting agent, to be used e.g. in cementing prosthetic crowns.

3.5. Surface roughness

Measurements of surface roughness were carried out according to the ISO 4288 standard, which is typically applied for the evaluation of roughness via the contact method. A contact profilometer was used for the characterization and for each sample the Ra, Rt and Rz values were established (Table S5, Supplementary materials). As can be seen, the addition of diatomaceous earth in the tested model GIC resulted in alteration of its surface roughness parameters. A statistically significant difference was seen between the control and the DE-modified samples for Ra, Rt and Rz (Fig. 4).

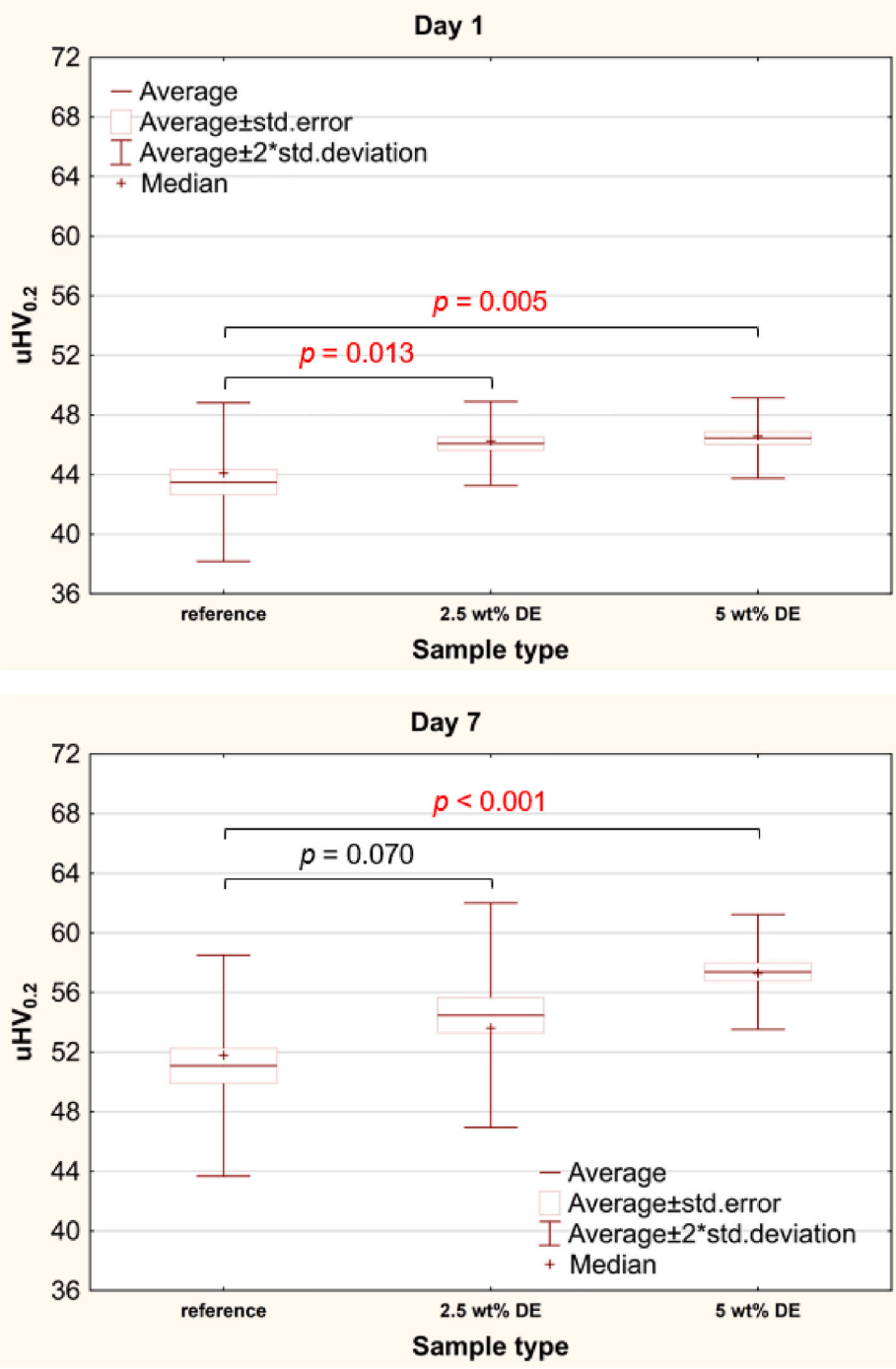

Fig. 2. Results of Vickers microhardness tests for samples conditioned in deionized water, 37 °C, for 1 or 7 days.

3.6. Tribological performance

Upon completing the aforementioned tests, the influence of DE addition on the frictional and wear properties of the tested GIC was assessed. Typically, during these measurements, the average value of friction force *F*, as well as the volumetric wear of the samples, is measured (Table S6, Supplementary materials). It was noticed that with increasing content of the diatomite in the GIC, the average friction force changed from 2.54 (control) to 2.49 (2.5 wt% DE) and 2.45 (5 wt% DE) (Fig. S4, Supplementary materials). However, under the tested conditions, no statistically significant effect on the *F* was seen when DE was incorporated in the GIC, regardless of the DE content. The observed values of the friction force translated also into volumetric wear of the materials, revealing no effect on the wear performance, under the testing conditions, of the tested GICs containing DE filler (Fig. S5, Supplementary materials). The presented tribological data is well supported by the microscopic observations. Exemplary friction tracks obtained on both the control group (0 wt% DE) and the DE-filled samples revealed a regular, elliptical shape of the wear scar (Fig. 5a and b). Numerous pores were also visible. However, these were not formed as a result of friction. Moreover, some cracks were noticeable in both regions: the wear track, as well as in the adjacent area. Apparently, far fewer cracks were noticed in the case of CLSM imaging (Fig. S6, Supplementary materials). This microscopic image of the wear track was taken while high relative humidity was maintained in the vicinity of the GIC sample. It is assumed that the appearance of most of the cracks of

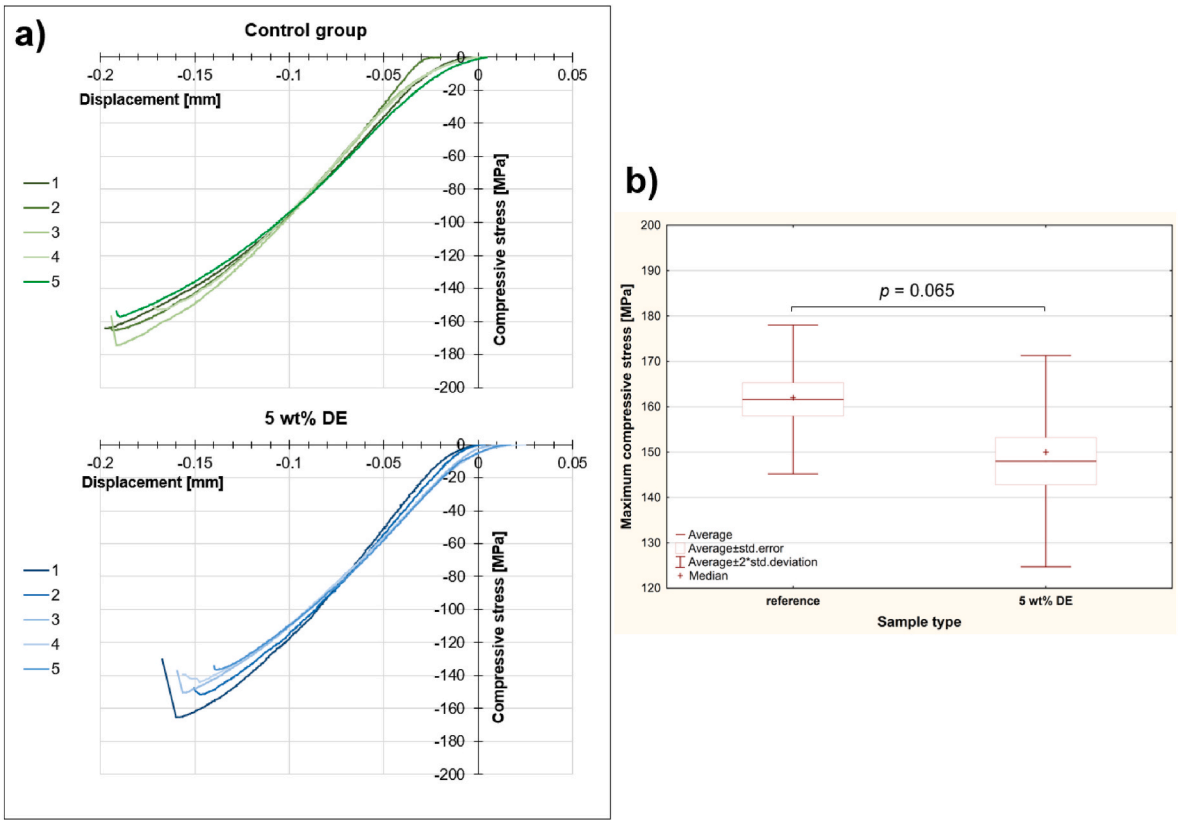

Fig. 3. Results of compressive strength tests, performed according to ISO 9917–1: (a) the compressive stress – displacement curves, observed for the reference and 5 wt% DE-filled samples; (b) boxplots presenting distribution of the obtained data.

the GIC could be attributed strictly to the SEM technique, which required a high vacuum, causing rapid removal of the solvent from the hydrogel matrix. The damaging effect of the vacuum is well seen when Fig. 5 is compared with Fig. S6. However, it has to be noted that only in the reference sample (Fig. 5a), semi-circular cracks were seen on the worn surface. These cracks resulted from the accumulation of tensile stress in front of the ball during reciprocating movement.

To obtain a better insight into the microstructure and the dominant wear modes of the tested GICs, high magnification images of the wear tracks were taken using SEM. First of all, in a reference sample (series 1), the surface heterogeneity of the wear scar is noticeable (Fig. 6a). A hydrogel matrix (Fig. 6a, red arrows) in which the glass particles are present (yellow and blue circles) is seen in the tested GIC. The glass particles differ in morphology, which is a consequence of the different types of reinforcement particles used within the commercial formulation. The manufacturer also ensures material impermeability to X-rays. Therefore, the bright spots visible on the cross-section of the glass particle are nanoparticles that contain heavy elements (radiocontrast agents). As a result of wear, some of the nanoparticles were released from the glass and became embedded in the matrix (Fig. 6a, violet arrows).

However, the morphology of the wear track changed substantially when diatomaceous earth particles were incorporated in the GIC (Fig. 6c). The wear products, which were mixed with the free glass particles, tended to form spall-like structures that resembled sites being plasticly deformed as a consequence of friction (Fig. 6c). Therefore, compared with the reference sample (Fig. 6a), it can be claimed that the addition of DE particles in the glass-ionomer cements resulted in modification of the dominant wear modes under frictional conditions. Moreover, it can be seen that the DE frustules tended to become damaged due to wear (Fig. 6d). The contact site of the frustule with the counter sample (corundum ball) became flattened. In fact, it was also evidenced that the GIC penetrates the cavities of the frustules.

4. Discussion

In this study, a set of null hypotheses on the lack of influence of the addition of diatomaceous earth on the crucial performance properties, that is: surface microhardness ($H_{0\text{-}1}$), compressive strength ($H_{0\text{-}2}$), film thickness ($H_{0\text{-}3}$), surface roughness ($H_{0\text{-}4}$), and tribological performance ($H_{0\text{-}5}$), was tested. The listed hypotheses were tested against the alternative hypotheses of a difference ($H_{A\text{-}1}$ to $H_{A\text{-}5}$). According to the results, some of the null hypotheses had to be rejected due to $p > 0.05$, that is: $H_{0\text{-}1}$, $H_{0\text{-}3}$, and $H_{0\text{-}4}$. Therefore, the alternative hypotheses of difference: $H_{A\text{-}1}$, $H_{A\text{-}3}$, and $H_{A\text{-}4}$, were accepted.

It should be noted that as soon as the glass powder is in contact with the polymeric fluid, a setting reaction starts. The working time does not exceed 180 s for most conventional GICs. Therefore, the hand-mixed version of Ketac Molar Easymix was selected, as the purpose of the study is to test the influence of DE addition on the performance of a GIC. It is easy to incorporate DE in the mixture. Moreover, the weight powder to liquid ratio (PTLR) was fixed at 3.1:1 for the tested GIC, which corresponds to the 0.69 PTLR ratio recommended by the manufacturer. It was decided to reduce the amount of powder, as it was planned to test the influence of substituting part of the glass powder with a bio-derived filler – diatomaceous earth. Obviously, the powder to liquid ratio affects the performance of the resultant GIC.

The microhardness test revealed an increase of the average reported surface microhardness of the reference samples obtained (Fig. 2) from 43.5 HV (1 day of conditioning) to 51.1 HV (7 days of conditioning), which correlates with the results obtained by other authors (Silva et al., 2007a; Lima et al., 2019). However, one has to be aware that the direct comparison of the surface microhardness with the values reported by other authors is challenging, as in most published works both the

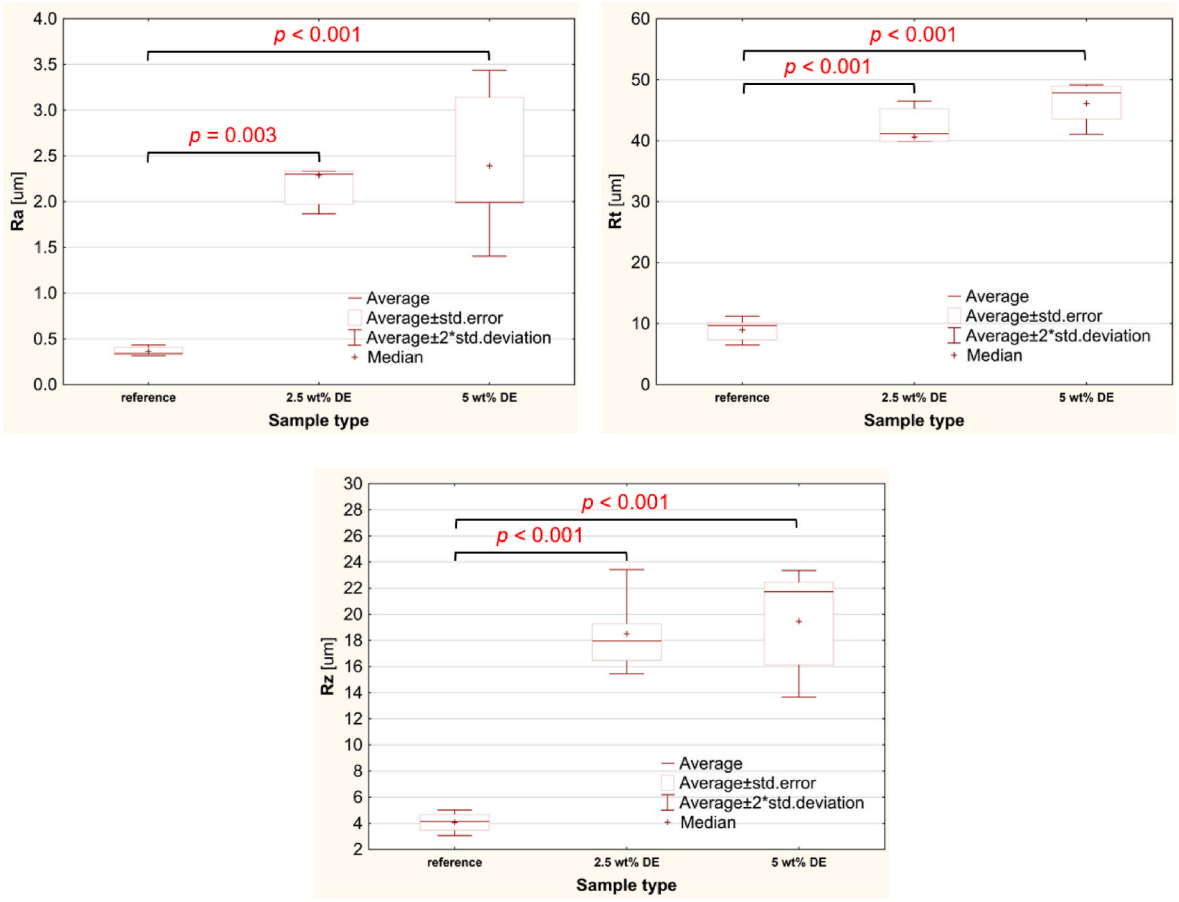

Fig. 4. Results of surface roughness measurements performed according to ISO 4288.

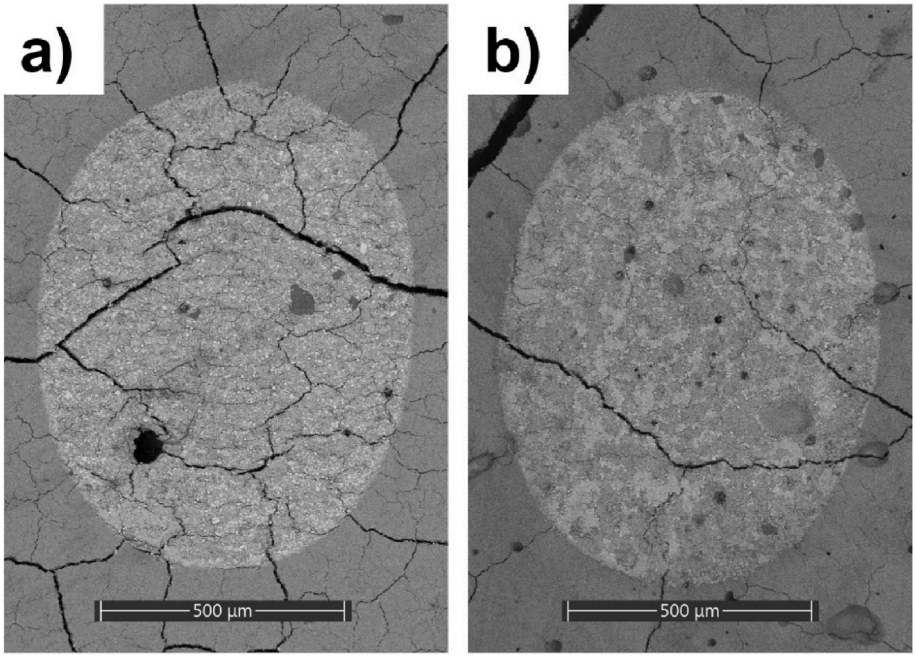

Fig. 5. Microstructures of the wear tracks obtained on: (a) control, and (b) 5 wt% DE filled glass-ionomer samples. The images were taken with SEM, using an in-lens backscatter electron (BSE) detector.

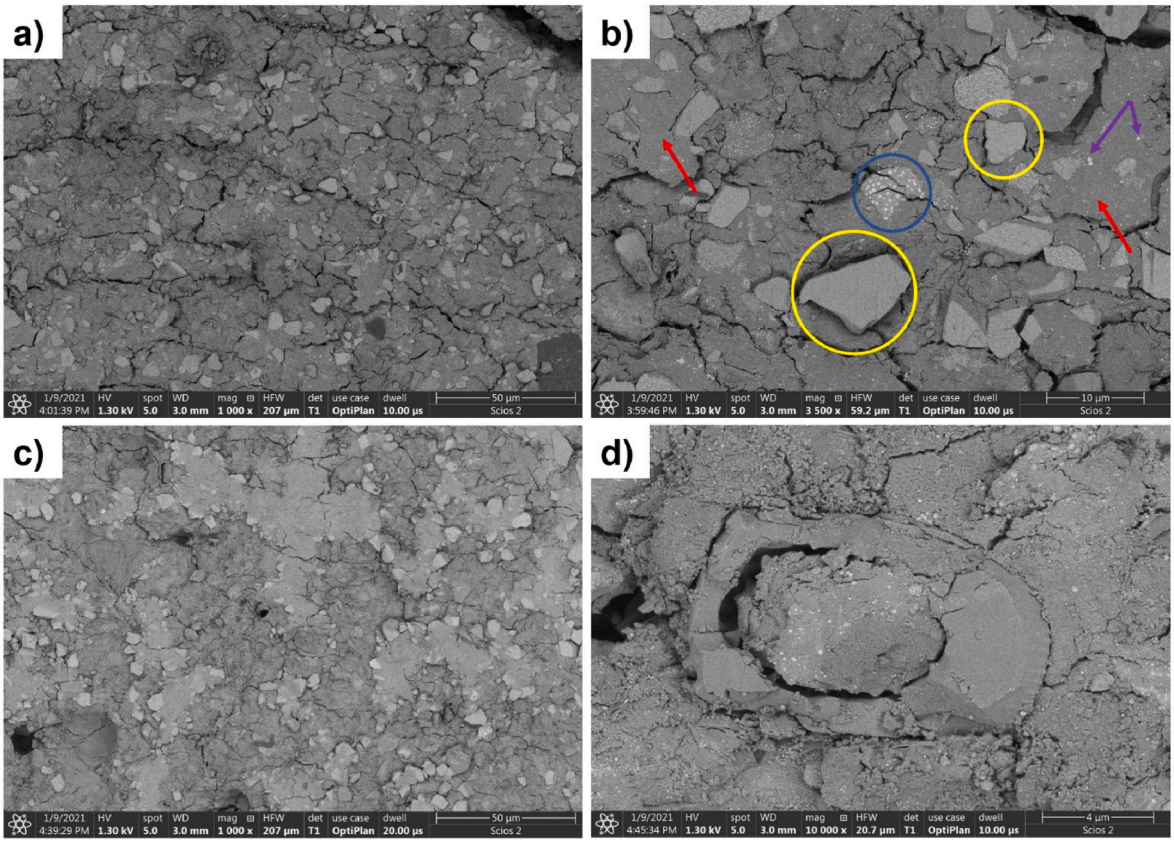

Fig. 6. High magnification images of the wear tracks presented in Fig. 5: (a)–(b) control, magnifications 1000 × and 3500 × ; (c)–(d) 5 wt% DE, magnifications 1000 × and 10000 × . The images were taken with SEM, using an in-lens backscatter electron (BSE) detector.

methods for surface hardness testing and the test conditions differ (Oliveira et al., 2021; de Lima Navarro et al., 2021; Youn-Soo, 2015; Bonif á cio et al., 2009), which can significantly affect the results. On the other hand, some authors reported higher surface hardness of Ketac Molar Easymix under the same measurement conditions as proposed in our study (Gill and Pathak, 2010). Another issue is that the weight ratio of powder to liquid was decreased compared to the manufacturer's recommendation, which could affect the resultant microhardness of the control group. Nevertheless, it can be concluded that the addition of 5 wt % DE provides a statistically significant increase in the surface hardness of the tested glass-ionomer cement (Fig. 2). This should be an advantage considering the projected *in vivo* performance of the tested composition, as the surface hardness is directly proportional to the wear performance of the material. A substantial increase in the surface hardness of glass-ionomer cements after introducing various types of micro- and nanoparticles, including Ketac Molar Easymix, was reported also by other authors, e.g. (Cibim et al., 2017). The observed effect on the surface hardness of the tested GIC can be attributed to the strengthening by diatoms frustules, which can quantitatively be described by a rule of mixtures (Kim, 2000). The frustules found in diatomaceous earth contain almost pure silica (Delasoie and Zobi, 2019; Aw et al., 2012, 2013); however, they show high resistance to deformation because of their unique architecture. A similar strengthening effect of the frustules on the polymeric matrix composites was reported also in (Wang et al., 2011), where the diatomite particles were used as a reinforcement in the Bis-GMA-TEGDMA matrix.

On the other hand, considering compressive strength, no statistically significant difference was noticed between the reference and the DE-containing samples (Fig. 3b). Considering the projected application of DE in GICs, that is, the drug-carrying and releasing agent, the absence of any weakening effect on the compressive strength of the material is an advantage. However, comparison of the data obtained with other authors is challenging. In numerous works, instead of providing compressive stress, the compressive force is given (Koenraads et al., 2009; Molina et al., 2013). Considering variability in the sample dimensions, the compressive force does not provide sufficient information on the performance of the material when loaded under compression. On the other hand, in one work (Kantovitz et al., 2020), the average reported compressive strength of KME was 89.46 MPa. It should be noted that the reported value is significantly lower than the results obtained in this study (Fig. 3b). However, the value of 89.46 MPa would suggest that the material does not meet the requirements stated in the ISO 9917-1 standard, where out of 5 tested samples at least 4 should present a maximum compressive strength of at least 100 MPa. However, in other studies (Peez and Frank, 2006; Shiozawa et al., 2014; Silva et al., 2007b), it was revealed that after 24 h of setting, the compressive strength of KME tested according to ISO 9917–1 fluctuates between 133 and 230 MPa. Therefore, it is suspected that the reported dispersion in data presented by other research groups may be caused by the different protocols of samples preparation, particularly difficulties related to uniform mixing by the operators. In fact, this concern was raised also by other authors (Koenraads et al., 2009). According to the manufacturer's recommendation, the mixing time of KME should not exceed 30 s (Koenraads et al., 2009). It is challenging to obtain a homogeneous mixture within such a short time span, especially if a greater amount of material is required to prepare samples for mechanical tests. Moreover, the number of internal voids, e.g. pores originating from entrapped air bubbles, is difficult to control when the hand-mixed version is used. The number of voids is directly correlated with the performance of a glass-ionomer under compression – the more voids there are, the lower the compressive strength is (Arnold, 2019). It was shown that a slightly lower compressive strength of 3M's Ketac Molar is obtained when the material is mixed by hand instead of centrifuging (Nomoto and McCabe, 2001). A similar trend was reported also in (Arnold, 2019).

As evidenced in Fig. 4, the surface roughness, as determined by Ra, Rt and Rz (measured according to ISO 4288), increases after introducing DE into the glass-ionomer matrix. This can be attributed to the morphology of *Aulacoseira* frustules (Fig. 1), which are larger than the glass particles (Fig. 1c, d). Their presence in the matrix results in greater differences in the height of bulges/dents on the surface of the composite.

From the perspective of a clinical application of the proposed material, the increased surface roughness of the restored tooth surface causes the accumulation of plaque, secondary caries, gingivitis and loss of periodontal attachment (Warren et al., 2002). According to research by Bollen et al. (1996) on implant materials, the critical Ra for oral bacteria colonization is 0.2 μm. In the case of DE-filled GIC, all the tested series, including the reference, revealed Ra which is much higher (Fig. 4). However, it has to be noted that prior to surface roughness measurements, the samples were not subjected to any surface treatment, e.g. polishing or varnishing. In one study (Warren et al., 2002), it was presented that the surface roughness of restorative materials, including GICs, can be substantially reduced after polishing with prophylaxis pastes. However, according to other authors (Mili č evi ć et al., 2018), in comparison with machine finishing and polishing, the lowest achievable surface roughness in GICs is obtained when a Mylar strip is used for the surface finish. In our case, instead of a Mylar foil, a polypropylene foil was used to secure the samples during the first hour of setting. Nevertheless, in the work by Perez et al. (2009), the authors stated that, compared with the Mylar foil, the lowest surface roughness in GICs is achieved when the Sof-Lex polishing system (3M Dental Products) is used. Therefore, there is no unequivocal opinion in the scientific community on the best surface finish method applicable for GICs. Considering DE-loaded GICs, it seems that their surface roughness may be higher than that of the reference. However, based on the literature information provided above, it is assumed that the surface roughness might be substantially reduced by mechanical grinding or polishing with particles smaller than the size of the frustules. This hypothesis is well supported by the microscopic observations of the wear tracks (Fig. 6c, d), where abrasive flattening of the frustules is seen as a result of friction. Therefore, it can be expected that the surface roughness can be substantially reduced after the mechanical surface treatment, reducing the height of the frustules protruding from the surface of the specimens. Surface treatment of the composites to reduce their roughness is a subject of ongoing research.

The surface roughness of the material, as well as its microhardness, are directly related to its tribological properties. In general, the greater is the surface microhardness and the lower the roughness, the better. However, even though a statistically significant difference in surface microhardness (Fig. 2) or roughness (Fig. 4) is present between the tested sample series, no difference is noticed in tribological studies. In both the friction force (Fig. S4) and volumetric wear (Fig. S5) measurements, the statistical analysis performed did not reveal a difference in the frictional and wear performance between the reference and the DE-loaded samples.

The proposed tribological study was designed with respect to the relevant literature in the field. Therefore, as the first step, the lubricating conditions had to be carefully selected. According to (Zheng et al., 2022), one of the factors which contributes to the prevention of wear in the oral environment is the type and content of mucins present in human saliva. Therefore, instead of using typical solutions such as Ringer's or phosphate-buffered saline (PBS) as simulated body fluids, in this study the tribological pair was lubricated with a commercial artificial mucin-rich saliva, Kserostemin (Aflofarm; Pabianice, Poland). A similar approach, based on using a mucin-rich lubricant for wear testing of restorative materials, was proposed also in the literature (Kielbassa et al., 2021). The selected protocol made the lubrication conditions mimic those present in the human oral cavity. Considering the design of a tribological study, also the load, length of the wear track, and the duration of one respective movement have to be carefully chosen, in order to make the frictional studies clinically relevant. Therefore, in some works, chewing simulators are used, and the tested restorative materials are placed in model acrylic teeth. A natural movement of the mandible is replicated, while the four translative motions are simulated (Kielbassa et al., 2021). Sometimes, also oscillating movements in a pin-on-block design are chosen (Zantner et al., 2004). However, in most published works on the tribological performance of dental materials, e.g. (Villat et al., 2014; Walczak and Drozd, 2016; Dziedzic et al., 2016), a circular wear track of a specific radius is selected. Typically, the selected normal load in this configuration varies between 1 and 10 N. On the other hand, as a counter sample, irrespective of the frictional configuration, an alumina ball is chosen (Zantner et al., 2004; Villat et al., 2014; Walczak and Drozd, 2016; Dziedzic et al., 2016).

However, taking into account the clinical relevance of the results and the actual working conditions of a GIC that occur during mastication, in our study, we selected fretting-like frictional conditions. In fact, it was presented that, in occlusion, the relative movement of the incisor point in the sagittal plane equals approx. 0.2 mm for hard food and 0.1 mm for soft food, while in the frontal trajectory, it typically does not exceed 1 mm, irrespective of the hardness of the masticated food (Xu et al., 2008). On the other hand, it was shown that teeth tend to move by around 0.1 mm not only when loaded but also when they remain without direct occlusal contact (Bando et al., 2009). Therefore, we selected the length of the wear track as 0.5 mm. At this length of the wear track, the normal load of 5 N was applied. It was shown in the literature that the load applied on a single tooth during chewing ranges between 70 and 150 N, while the maximum biting force that can be applied to molars measures up to 700 N (Xu et al., 2008). However, it has to be noted that this load is transferred on teeth via occlusal surfaces. It is estimated that the mean occlusal surface area in humans is 739 mm^2 (Bourdiol and Mioche, 2000). Therefore, a normal load amounting to even a few thousands of Newtons is being uniformly transferred on the whole contacting area equal to the average of 739 mm^2. On the other hand, in the testing configuration proposed by us, the load of 5 N was transferred to the GIC via point contact – that is, when divided by the contact surface, the contact pressure exceeded the one present in human teeth. Moreover, it is estimated that the duration of one chewing cycle varies from 0.87 to 0.95 s (Pr ö schel and Hofmann, 1988). Considering this information, the frequency of movement of the ball on the GIC disk was set to 1 Hz. A similar frequency of oscillational movements was proposed also in (Kielbassa et al., 2021).

To sum up the discussion on the tribological performance of the proposed composite materials, no effect of the diatom frustules on the tribological performance of the tested GIC was observed in the selected testing conditions. Taking into account the fact that the prospective purpose of substituting part of the glass powder with DE is to provide a drug-loaded carrier which, at the same time, will make it possible to reduce the retail price of the final product, the absence of any effect on the frictional and wear behavior of GIC is an advantage. However, it has to be noted that, compared with the reference (Fig. 6a), the dominant wear mode changes when DE is introduced into the GICs hydrogel matrix (Fig. 6c). Nevertheless, it does not affect the resultant volumetric wear (Fig. S5) or the resistance to motion (Fig. S4) in a model frictional couple of GIC vs. an alumina ball.

While the results obtained in this study seem promising, one has to be aware of the limitations that arise from the design of the experiment. Above all, this was a preliminary work, focused on determining the applicability of the addition of diatomaceous earth in conventional glass-ionomer cements. Therefore, the tests conducted, in which an attempt to determine the influence of DE on the crucial performance properties on a model GIC was undertaken, had a comparative character. Their purpose was to measure the baseline properties of the proposed composite material under model, laboratory conditions. As a consequence, surface microhardness and roughness, compressive strength, film thickness and tribological performance were selected as the properties that are crucial from the perspective of the future application of the composite. As presented, the proposed composite cannot be

applied as a crown and bridge cementing agent, as the produced film thickness is far too high. Nevertheless, the combination of high surface hardness, good tribological properties, and high viscosity make the obtained material a promising candidate for permanent restorations in children who need atraumatic restorative treatment (ART). In previous studies, it was shown that loading GICs with antibiotics can successfully be used in children to seal off the caries-infected dentin (Ferreira et al., 2013). Therefore, the introduction of the drug-releasing agent (DE) in GICs for ART may improve the clinical outcome of this kind of treatment. Moreover, substituting part of the glass with diatomite will positively affect the final price of the dental product, indirectly improving the availability of dental care in developing countries. However, in this study, in the surface roughness measurements, the as-received samples were used instead of the specimens that were earlier subjected to mechanical surface finish. This was done in order to assess the basic influence of the DE addition on the composite surface topography obtained. Nevertheless, as a next step, it is necessary to perform additional research, where the impact of the various surface finish techniques on the resultant surface roughness of the DE-loaded glass--ionomers will be tested. It seems that the optimal surface finish method may be selected only based on empirical results.

5. Conclusions

In this study, the effect of substituting part of the glass powder with diatomaceous earth particles on the performance of a conventional glass-ionomer cement is discussed. The resultant surface microhardness and roughness, wear performance, compressive strength, and film thickness of the DE-modified cement (GIC) were tested. Based on the obtained data, the following conclusions are put forward:

1. Considering the promising application of diatomaceous earth as a drug-loaded carrier in GICs, the observed effect of the DE on the performance of the proposed composite material is favorable. It was shown that the DE can effectively substitute part of the glass particles in the tested GIC without deterioration of its crucial properties, including surface microhardness, compressive strength and tribological performance. From the clinical point of view, it seems that the proposed composite may be a promising candidate for ART restorations.
2. Compared with the tested model, the DE-modified GIC possesses greater surface roughness. However, it needs to be stated clearly that the prepared samples were not subjected to any kind of mechanical processing, e.g. grinding or polishing. Therefore, as a next step, it is advisable to develop a surface preparation method to reduce the surface roughness.

CRediT authorship contribution statement

Magdalena Łępicka: Writing – review & editing, Writing – original draft, Visualization, Validation, Methodology, Investigation, Formal analysis, Data curation, Conceptualization. **Magdalena Rodziewicz:** Writing – original draft, Investigation. **Michał Kawalec:** Writing – review & editing, Writing – original draft, Supervision, Resources, Project administration, Formal analysis, Conceptualization. **Klaudia Nowicka:** Investigation. **Yurii Tsybrii:** Investigation, Data curation. **Krzysztof Jan Kurzydłowski:** Writing – review & editing, Supervision, Project administration, Funding acquisition, Conceptualization.

Declaration of competing interest

The authors declare that they have no known competing financial interests or personal relationships that could have appeared to influence the work reported in this paper.

Data availability

Data will be made available on request.

Acknowledgments

This work was financially supported in the frame of the project “Advanced Biocomposites for Tomorrow’s Economy BIOG-NET”, FNP POIR.04.04.00-00-1792/18–00. The project is carried out within the TEAM-NET program of the Foundation for Polish Science, co-financed by the European Union under the European Regional Development Fund. Professional profreading of the paper was financed from the funds of Department of Materials Science and Production, Faculty of Mechanical Engineering, Bialystok University of Technology, Poland, project no. WZ/WM-IIM/2/2020.

Appendix A. Supplementary data

Supplementary data to this article can be found online at https://doi.org/10.1016/j.jmbbm.2022.105324.

References

Ahmad, F.J., Iqbal, Z., Jain, N., Jain, G.K., Talegaonkar, S., Ahuja, A., et al., 2008. Dental therapeutic systems. Recent Pat. Drug Deliv. Formulation 2 (1), 58–67.
Arnold, S., 2019. Comparative Evaluation of the Compressive Strength Surface Hardness and Porosity of a Selection of Capsule-Mixed versus Hand-Mixed Glass Ionomer Cements. University of Pretoria, Pretoria, South Africa.
Aw, M.S., Simovic, S., Yu, Y., Addai-Mensah, J., Losic, D., 2012. Porous silica microshells from diatoms as biocarrier for drug delivery applications. Powder Technol. 223, 52–58.
Aw, M.S., Bariana, M., Yu, Y., Addai-Mensah, J., Losic, D., 2013. Surface-functionalized diatom microcapsules for drug delivery of water-insoluble drugs. J. Biomater. Appl. 28 (2), 163–174.
Bando, E., Nishigawa, K., Nakano, M., Takeuchi, H., Shigemoto, S., Okura, K., et al., 2009. Current status of researches on jaw movement and occlusion for clinical application. Jpn Dent Sci Rev 45 (2), 83–97.
Bollen, C.M., Papaioanno, W., Van Eldere, J., Schepers, E., Quirynen, M., Van Steenberghe, D., 1996. The influence of abutment surface roughness on plaque accumulation and peri-implant mucositis. Clin. Oral Implants Res. 7 (3), 201–211.
Bonifácio, C., Kleverlaan, C., Raggio, D., Werner, A., De Carvalho, R., Van Amerongen, W., 2009. Physical-mechanical properties of glass ionomer cements indicated for atraumatic restorative treatment. Aust. Dent. J. 54 (3), 233–237.
Bourdiol, P., Mioche, L., 2000. Correlations between functional and occlusal tooth-surface areas and food texture during natural chewing sequences in humans. Arch. Oral Biol. 45 (8), 691–699.
Cibim, D.D., Saito, M.T., Giovani, P.A., Borges, A.F.S., Pecorari, V.G.A., Gomes, O.P., et al., 2017. Novel nanotechnology of TiO2 improves physical-chemical and biological properties of glass ionomer cement. Int J Biomater 2017.
de Lima Navarro, M.F., Pascotto, R.C., Borges, A.F.S., Soares, C.J., Raggio, D.P., Rios, D., et al., 2021. Consensus on glass-ionomer cement thresholds for restorative indications. J. Dent. 107, 103609.
Delasoie, J., Zobi, F., 2019. Natural diatom biosilica as microshuttles in drug delivery systems. Pharmaceutics 11 (10), 537.
Dziedzic, K., Zubrzycka-Wróbel, J., Józwik, J., Barszcz, M., Siwak, P., Chałas, R., 2016. Research on tribological properties of dental composite materials. Adv Sci Technol Res J 10 (32), 144–149.
Ersin, N.K., Candan, U., Aykut, A., Eronat, C., Kose, T., 2006. A clinical evaluation of resin-based composite and glass ionomer cement restorations placed in primary teeth using the ART approach: results at 24 months. J Am Dent Assoc 137 (11), 1529–1536.
Ferreira, J.M.S., Pinheiro, S.L., Sampaio, F.C., Menezes, VAd, 2013. Use of glass ionomer cement containing antibiotics to seal off infected dentin: a randomized clinical trial. Braz. Dent. J. 24, 68–73.
Ficai, D., Sandulescu, M., Ficai, A., Andronescu, E., Yetmez, M., B Agrali, O., et al., 2017. Drug delivery systems for dental applications. Curr. Org. Chem. 21 (1), 64–73.
Fisher, J., Varenne, B., Narvaez, D., Vickers, C., 2018. The Minamata Convention and the phase down of dental amalgam. Bull. World Health Organ. 96 (6), 436.
Gao, W., Smales, R., Yip, H., 2000. Demineralisation and remineralisation of dentine caries, and the role of glass-ionomer cements. Int. Dent. J. 50 (1), 51–56.
Gill, N., Pathak, A., 2010. Comparative evaluation of the effect of topical fluorides on the microhardness of various restorative materials: an in vitro study. J Indian Soc Ped Prev Dent 28 (3), 193.
Kantovitz, K.R., Fernandes, F.P., Feitosa, I.V., Lazzarini, M.O., Denucci, G.C., Gomes, O. P., et al., 2020. TiO2 nanotubes improve physico-mechanical properties of glass ionomer cement. Dent. Mater. 36 (3), e85–e92.
Khvostenko, D., Mitchell, J., Hilton, T., Ferracane, J., Kruzic, J., 2013. Mechanical performance of novel bioactive glass containing dental restorative composites. Dent. Mater. 29 (11), 1139–1148.

Khvostenko, D., Hilton, T., Ferracane, J., Mitchell, J., Kruzic, J., 2016. Bioactive glass fillers reduce bacterial penetration into marginal gaps for composite restorations. Dent. Mater. 32 (1), 73–81.
Kielbassa, A.M., Glockner, G., Wolgin, M., Glockner, K., 2016. Systematic review on highly viscous glass-ionomer cement/resin coating restorations (Part I): do they merge Minamata Convention and minimum intervention dentistry? Quintessence Int. 47 (10).
Kielbassa, A.M., Glockner, G., Wolgin, M., Glockner, K., 2017. Systematic review on highly viscous glass-ionomer cement/resin coating restorations (Part II): do they merge Minamata Convention and minimum intervention dentistry? Quintessence Int. 48 (1).
Kielbassa, A.M., Oehme, E.P., Shakavets, N., Wolgin, M., 2021. In vitro wear of (resin-coated) high-viscosity glass ionomer cements and glass hybrid restorative systems. J. Dent. 105, 103554.
Kim, H.S., 2000. On the rule of mixtures for the hardness of particle reinforced composites. Mater Sci Eng A 289 (1–2), 30–33.
Kiss, K., Klee, R., Ector, L., Acs, E., 2012. Centric diatoms of large rivers and tributaries in Hungary: morphology and biogeographic distribution. Acta Bot. Croat. 71 (2), 311–363.
Koenraads, H., Van der Kroon, G., Frencken, J., 2009. Compressive strength of two newly developed glass-ionomer materials for use with the Atraumatic Restorative Treatment (ART) approach in class II cavities. Dent. Mater. 25 (4), 551–556.
Lavigueur, C., Zhu, X., 2012. Recent advances in the development of dental composite resins. RSC Adv. 2 (1), 59–63.
Liang, J., Peng, X., Zhou, X., Zou, J., Cheng, L., 2020. Emerging applications of drug delivery systems in oral infectious diseases prevention and treatment. Molecules 25 (3), 516.
Lima, R.B.W.E., De Vasconcelos, L.C., Pontual, M.L., Meireles, S.S., Andrade, A.K.M., Duarte, R.M., 2019. Effect of ionizing radiation on the properties of restorative materials. Indian J. Dent. Res. 30 (3), 408.
Lohbauer, U., 2009. Dental glass ionomer cements as permanent filling materials?—properties, limitations future trends. Materials 3 (1), 76–96.
Makvandi, P., Josic, U., Delfi, M., Pinelli, F., Jahed, V., Kaya, E., et al., 2021. Drug delivery (nano) platforms for oral and dental applications: tissue regeneration, infection control, and cancer management. Adv. Sci. 8 (8), 2004014.
Matsuya, S., Matsuya, Y., Ohta, M., 1999. Structure of bioactive glass and its application to glass ionomer cement. Dent. Mater. J. 18 (2), 155–166.
Miličević, A., Goršeta, K., van Duinen, R.N., Glavina, D., 2018. Surface roughness of glass ionomer cements after application of different polishing techniques. Acta Stomatol. Croat. 52 (4), 314–321.
Molina, G.F., Cabral, R.J., Mazzola, I., Lascano, L.B., Frencken, J.E., 2013. Mechanical performance of encapsulated restorative glass-ionomer cements for use with Atraumatic Restorative Treatment (ART). J. Appl. Oral Sci. 21, 243–249.
Nomoto, R., McCabe, J.F., 2001. Effect of mixing methods on the compressive strength of glass ionomer cements. J. Dent. 29 (3), 205–210.
Oliveira, L., Dos Santos, P., Ramos, F., Moda, M., Briso, A., Fagundes, T., 2021. Wear, roughness and microhardness analyses of single increment restorative materials submitted to different challenges in vitro. Eur. Arch. Paediatr. Dent. 22 (2), 247–255.
Peez, R., Frank, S., 2006. The physical–mechanical performance of the new Ketac™ Molar Easymix compared to commercially available glass ionomer restoratives. J. Dent. 34 (8), 582–587.
Perez, CdR., Hirata Jr., R., Silva, A., Sampaio, E., Miranda, M., 2009. Effect of a glaze/composite sealant on the 3-D surface roughness of esthetic restorative materials. Oper Dent 34 (6), 674–680.
Pröschel, P., Hofmann, M., 1988. Frontal chewing patterns of the incisor point and their dependence on resistance of food and type of occlusion. J. Prosthet. Dent 59 (5), 617–624.
Prabhakar, A., Jibi Paul, M., Basappa, N., 2010. Comparative evaluation of the remineralizing effects and surface micro hardness of glass ionomer cements containing bioactive glass (S53P4): an in vitro study. Int J Clin Pediatr Dent 3 (2), 69.
Shiozawa, M., Takahashi, H., Iwasaki, N., 2014. Fluoride release and mechanical properties after 1-year water storage of recent restorative glass ionomer cements. Clin Oral Investig 18 (4), 1053–1060.
Silva, R., Zuanon, A.C.C., Esberard, R., Candido, M., Machado, J., 2007a. In vitro microhardness of glass ionomer cements. J. Mater. Sci. Mater. Med. 18 (1), 139–142.
Silva, R., Zuanon, A.C.C., Esberard, R., Candido, M., Machado, J., 2007b. In vitro microhardness of glass ionomer cements. J. Mater. Sci. Mater. Med. 18 (1), 139–142.
Sofan, E., Sofan, A., Palaia, G., Tenore, G., Romeo, U., Migliau, G., 2017. Classification review of dental adhesive systems: from the IV generation to the universal type. Ann. Stomatol. 8 (1), 1.
Villat, C., Ponthiaux, P., Pradelle-Plasse, N., Grosgogeat, B., Colon, P., 2014. Initial sliding wear kinetics of two types of glass ionomer cement: a tribological study. BioMed Res. Int. 2014.
Walczak, M., Drozd, K., 2016. Tribological characteristics of dental metal biomaterials. Curr. Issues Pharm. Med. Sci. 29, 158–162.
Wang, H., Zhu, M., Li, Y., Zhang, Q., Wang, H., 2011. Mechanical properties of dental resin composites by co-filling diatomite and nanosized silica particles. Mater. Sci. Eng. C 31 (3), 600–605.
Warren, D.P., Colescott, T.D., Henson, H.A., Powers, J.M., 2002. Effects of four prophylaxis pastes on surface roughness of a composite, a hybrid ionomer, and a compomer restorative material. J Esthet Restor Dent 14 (4), 245–251.
Worthington HV, Khangura S, Seal K, Mierzwinski-Urban M, Veitz-Keenan A, Sahrmann P, et al. Direct composite resin fillings versus amalgam fillings for permanent posterior teeth. Cochrane Database Syst. Rev. 2021 (8).
Xu, W., Bronlund, J., Potgieter, J., Foster, K., Röhrle, O., Pullan, A., et al., 2008. Review of the human masticatory system and masticatory robotics. Mech Mach Theory 43 (11), 1353–1375.
Youn-Soo, S., 2015. Effect of in-office bleaching application on the color, microhardness and surface roughness of five esthetic restorative materials. Indian J Sci Technol 8 (S1), 420–425.
Zantner, C., Kielbassa, A.M., Martus, P., Kunzelmann, K.-H., 2004. Sliding wear of 19 commercially available composites and compomers. Dent. Mater. 20 (3), 277–285.
Zheng, Y., Bashandeh, K., Shakil, A., Jha, S., Polycarpou, A.A., 2022. Review of dental tribology: current status and challenges. Tribol. Int. 166, 107354.